

## Preparation and Characterization of PAN-based Superfined Carbon Fibers for Carbon-paper Applications

Subong Kim, Yong Sik Chung, Heung-Soap Choi,<sup>†</sup> Fan-Long Jin,<sup>‡</sup> and Soo-Jin Park<sup>§,\*</sup>

Department of Organic Materials and Fiber Engineering, Chonbuk National University, Jeonju 561-756, Korea

<sup>†</sup>Department of Mechanical and Design Engineering, Hongik University, Sejong 339-701, Korea

<sup>‡</sup>Department of Polymer Materials, Jilin Institute of Chemical Technology, Jilin City 132022, People's Republic of China

<sup>§</sup>Department of Chemistry, Inha University, Nam-gu, Incheon 402-751, Korea. \*E-mail: sjpark@inha.ac.kr

Received August 25, 2013, Accepted September 23, 2013

Polyacrylonitrile (PAN)-based ultrafine fibers and carbon fibers were produced by wet-spinning, and the crystal sizes and thermal and mechanical properties of the fibers were investigated. Scanning electron microscopy revealed that the superfine fibrils in the surfaces of the PAN/polyvinyl acetate (PVA) blend fibers increased slightly with increasing PAN content before removal of the PVA. Differential scanning calorimetry indicated that the PAN and PVA in the blend fibers do not mix and, therefore, each maintains their inherent thermal characteristics. The crystal sizes of the blend fibers prepared by removing PVA with water increased at 5 wt % water. The extent of the reaction of the PAN carbon fibers, as calculated from the FT-IR spectra, is maximized at the stepwise temperature of 230 °C, and the density increased significantly above this temperature. The carbon fibers had relatively good mechanical properties, as shown by their tensile strength and modulus values of 2396 MPa and 213 GPa, respectively.

**Key Words :** Polyacrylonitrile, Ultrafine fibers, Carbon fibers, Crystal size, Tensile strength

### Introduction

Ultrafine fibers are defined as fibers that are finer than 0.7 denier; as a result, they have intrinsically ultrahigh specific surface areas. These fibers can be divided into filament and random staple forms.<sup>1,2</sup> To produce the fibers, polyacrylonitrile (PAN) and water-soluble polymers such as polyvinyl acetate (PVA) are homogeneously mixed in a common solvent and then wet-spun to form an "island-in-a-sea" type blend filament through phase separation of the polymers. The PAN ultrafine fibers, which have smaller fiber diameters and higher specific surface areas, are water-soluble and are thus obtained in the "sea" component. Their solubility in water is highly desirable for applications such as composite reinforcement, separation/filtration membranes, and surface-activated and surface-supported chemical reactions.<sup>3,4</sup>

Synthetic polymers, such as fibrils and ultrafine fibers, can improve the dispersion of carbon fibers in water, enhance bonding between the fibers to facilitate the preparation of paper, and affect the characteristics of the resultant papers, such as thickness, bulky density, and porosity. Ultrafine fibers prepared from PAN-based polymers are carbonized *via* oxidation stabilization and high-temperature heat treatment, which improve the density and strength of the final carbon fiber papers while maintaining their inherent electrical properties.<sup>5-8</sup>

The chemical reactions that occur during the oxidation stabilization process include cyclization, dehydrogenation, aromatization, oxidation, and cross-linking, and result in a conjugated ladder structure of the fibers. The resultant fibers have a thermally stable chemical structure and do not melt.

Carbonization usually occurs at 800-3000 °C, and the final products comprise 95% carbon. To further improve the properties of the carbon fibers, the fibers are graphitized at 1600-3000 °C. During this process, the carbon structure of the fibers is converted to a graphite structure. The graphitized carbon fibers comprise 99% carbon and have a very high elastic modulus.<sup>9-12</sup>

In this study, PAN ultrafine fibers and PAN carbon fibers were produced by wet-spinning. The fibers were characterized *via* scanning electron microscopy (SEM), differential scanning calorimetry (DSC), thermogravimetric analysis (TGA), X-ray diffraction (XRD), Fourier-transform infrared (FT-IR) spectroscopy, and universal testing.

### Experimental

**Materials.** PAN (12 K single tow) was purchased from Bluestar Co., Ltd. (China). PVA was supplied by Hyosung Co., Ltd. (Korea) and had a degree of polymerization of 2000 and degree of hydrolysis of 99%. Dimethyl sulfoxide (DMSO, 99%) and methyl alcohol (99.5%) were purchased from Samchun Chem. (Korea).

**Spinning of PAN/PVA Blend Fibers.** The concentrations of PAN and PVA were controlled at 18 and 15 wt %, respectively, by dissolution in DMSO, and the temperature was maintained at 50 °C. The PAN ultrafine fibers were produced by wet-spinning a PAN/PVA blend solution. The flow rate of the solution and jet stretch were 10 mL/min and 1.4, respectively. A mixture of methanol and water was used as the coagulating agent, and the temperature was maintained at 30 °C. The fibers were washed several times to completely

remove the solvent. The wet blend fibers were heat-treated to remove the PVA. Finally, the ultrafine fibers were prepared using a colloid mill.

**Spinning of Carbon Fibers.** The PAN carbon fibers were produced by wet-spinning a 15 wt % solution of PAN in DMSO. The flow rate of the PAN solution and jet stretch were 1 mL/min and 0.95, respectively. A mixture of methanol and water (50:50 wt %) was used as the coagulating agent. The fibers were washed several times to completely remove the solvent. The fibers were then heat-treated at 200–290 °C for 40–120 min. The fibers were carbonized at 700–1400 °C under a nitrogen atmosphere.

**Characterization and Measurements.** The morphologies of the PAN/PVA blend fibers before and after removal of the PVA were investigated *via* scanning electron microscopy (SEM, S-4700, Hitachi Ltd.).

The thermal properties of the fibers were investigated *via* differential scanning calorimetry (TA Q-series, TA Instruments) at a heating rate of 5 °C/min under a nitrogen atmosphere. The thermal decomposition of the fibers was studied *via* thermogravimetric analysis (Q-series, TA Instruments) at 35–600 °C with a heating rate of 20 °C/min under a nitrogen atmosphere.

The changes in the crystal structure were investigated using an X-ray diffraction analyzer (X'PERT MRD, Phillips) at 40 kV and 40 mA. The crystal size was calculated using the Scherrer equation, as follows:

$$L_c = \frac{K\lambda}{B\cos\theta} \quad (1)$$

where  $\lambda$  is the wavelength of the  $\text{CuK}\alpha$  irradiation (1.5418 Å),  $B$  is the full width at half maximum intensity,  $2\theta = 17^\circ$ , and  $K$  is a constant (0.89). The aromatization index (AI) was calculated using the following equation:

$$AI(\%) = \frac{I_a}{I_a + I_p} \times 100 \quad (2)$$

where  $I_a$  and  $I_p$  are the peak intensities at  $2\theta = 25.5$  and  $17^\circ$ , respectively.

Fourier-transform infrared spectra were recorded using a Thermo Nicolet AVATAR 370 spectrometer with the samples in the form of KBr pellets. The extent of reaction (EOR) was calculated using the following equation:

$$EOR = \frac{I_{1600}}{I_{CN} + I_{1600}} \quad (3)$$

where  $I_{1600}$  and  $I_{CN}$  are the peak absorption intensities at 1600 and 2240  $\text{cm}^{-1}$ , respectively.

The tensile properties were measured using a universal tester (5567A, Instron Co., USA) at a cross-head speed of 200 mm/min. All tensile properties were obtained by averaging seven experimental results.

## Results and Discussion

**Properties of Superfine PAN Fibers.** Figure 1 shows the morphologies of the PAN/PVA blend fibers as a function of

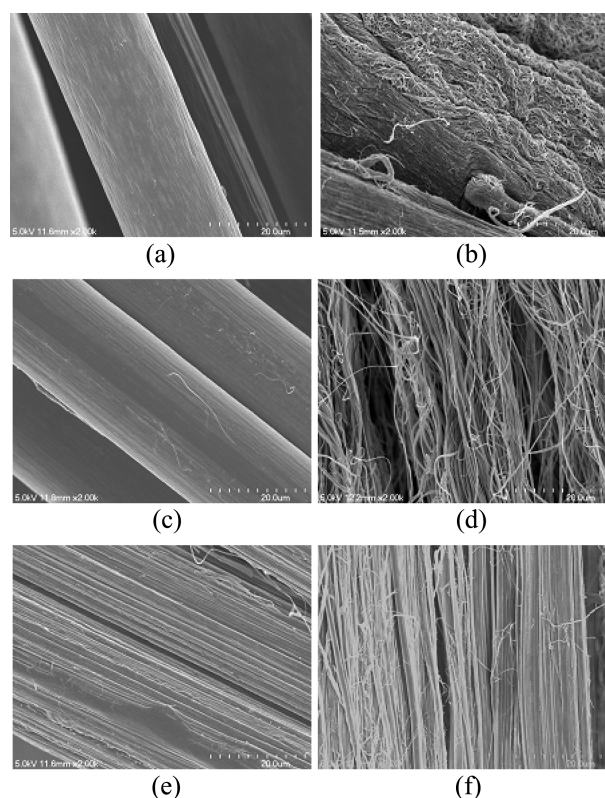


**Figure 1.** SEM images of PAN/PVA blend fibers before and after PVA removal: (a) 10 wt % PAN before PVA removal; (b) 10 wt % PAN after PVA removal; (c) 30 wt % PAN before PVA removal; (d) 30 wt % PAN after PVA removal; (e) 50 wt % PAN before PVA removal; (f) 50 wt % PAN after PVA removal.

the PAN/PVA composition. As shown in Figure 1(a), the superfine fibril content in the fiber surfaces increased slightly with increasing PAN content before PVA removal. The superfine fibers were split by the PAN fibrils when the PAN content was 50 wt %. The diameter of the superfine fibers decreased with decreasing PAN content after PVA removal; this trend is nonlinear and the order of the axis directions of the fibers is low, as shown in Figure 1(b). This is attributed to the greater shrinkage of the PAN superfine fibers induced by the decreased diameter of the fibers during the PVA removal process.<sup>13,14</sup>

Figure 2(a) shows DSC curves of the PAN/PVA blend fibers before PVA removal. The exothermic peak temperature of PAN and endothermic peak temperature of PVA were 289 and 235 °C, respectively. Increasing the PVA content from 10 to 50 wt % resulted in an increase in the exothermic peak temperature of PAN from 289 to 291 °C and decrease in the endothermic peak temperature of PVA from 235 to 233 °C. These results indicate that the PAN and PVA in the blend fibers do not mix; thus, each maintains their inherent thermal characteristics.<sup>15</sup>

Figure 2(b) shows DSC curves of the PAN/PVA blend fibers after PVA removal. The endothermic peak temperature of PVA at 230 °C disappeared, which indicates that the PVA was completely removed. Concomitantly, the exothermic peak temperature of PAN increase to 296–298 °C because of

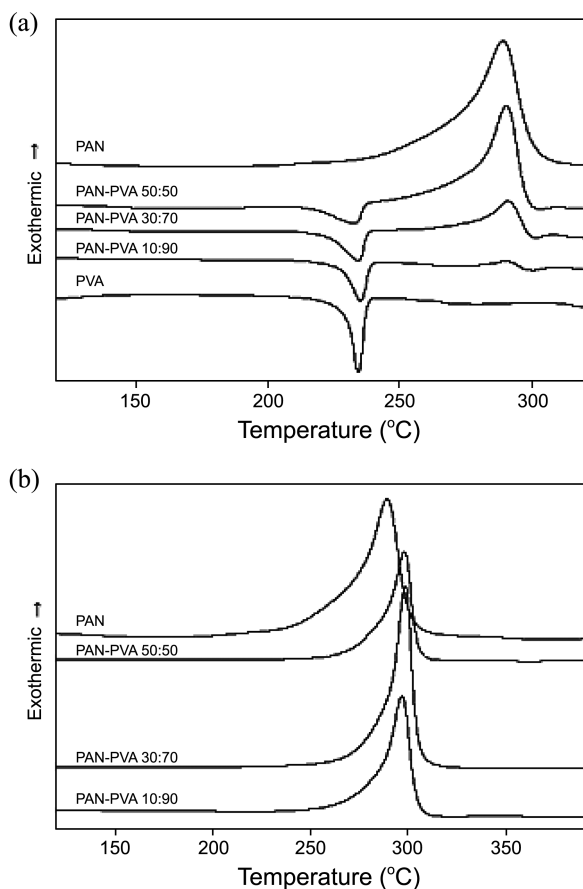


**Figure 2.** DSC curves of PAN/PVA blend fibers (a) before and (b) after PVA removal.

the removal of the PVA that was dissolved in water and permeated into the loose polymer chains of PAN fibers, which was induced by heat treatment.<sup>16</sup>

Figure 3 shows TGA curves of the PAN/PVA blend fibers. PVA underwent dramatic decomposition above 300 °C. However, the decomposition rate of thermally stabilized PAN is low. The char yield of the fibers at 600 °C increased gradually with increasing PAN content, which indicates that PAN and PVA did not mix and maintain their inherent

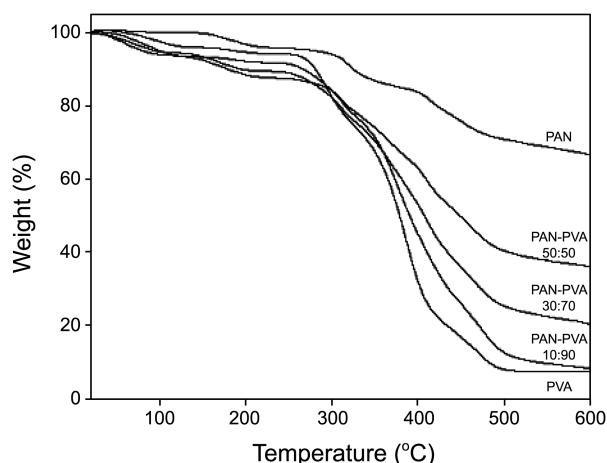


**Figure 3.** TGA thermograms of various fibers.

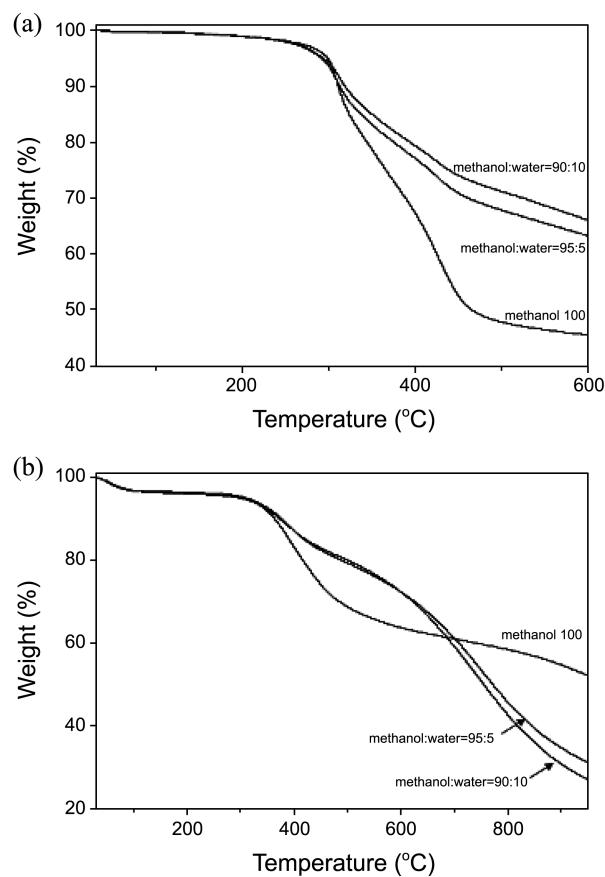


**Figure 4.** TGA curves of PAN/PVA (50:50) blend fibers on various coagulation bath systems (a) before and (b) after stabilization.

thermal characteristics; this supports the DSC results.<sup>17</sup>

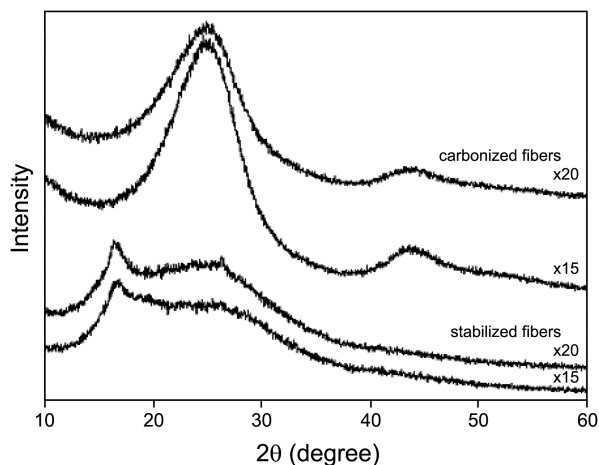
Figure 4 shows TGA curves of the PAN/PVA blend fibers in various coagulation bath systems before and after stabilization. As shown in Figure 4(a), the fiber prepared using only methanol decomposed significantly above 300 °C. When water was added to the coagulation bath, the decomposition rate of the fibers decreased, which indicates that the PVA was removed during spinning. The amount of PVA removed increased with increasing water content from 5 to 10 wt %.<sup>18</sup>

Figure 4(b) shows TGA curves of the PAN/PVA blend fibers after stabilization at 210–270 °C for 80 min. The fiber prepared using only methanol decomposed at about 345 °C and the final char yield was 50%. However, the fiber prepared after the addition of water to the coagulation bath had a greater than 70% char yield at 600 °C, and then decomposed significantly with increasing temperature until it reached a less than 30% char yield at 1000 °C. This is attributed to the dissolution of PVA in the water-containing coagulation bath: The PVA oligomer and water diffuse into PAN and remain in the fibril during spinning. The PVA oligomers in the polymer chains do not affect the chemical structure during stabilization; however, they hinder the bonding between the cyclized chains above 600 °C, which eventually leads to decomposition of the PAN fibers.<sup>19,20</sup>

Table 1 shows the XRD data for the PAN/PVA blend fibers prepared with water added to coagulation bath. The

**Table 1.** XRD data of PAN/PVA blend fibers with different coagulation bath systems

Water content (wt %)	Intensity at $2\theta \approx 17^\circ$ (CPS) <sup>a</sup>	Peak center ( $^\circ$ ) <sup>a</sup>	FWHM ( $^\circ$ ) <sup>a</sup>	Crystallite size (nm) <sup>a</sup>	AI (%) <sup>b</sup>
0	3597	16.94	1.204	1.191	54.53
5	3173	16.93	1.127	1.273	54.36
10	2780	16.88	1.208	1.187	55.02

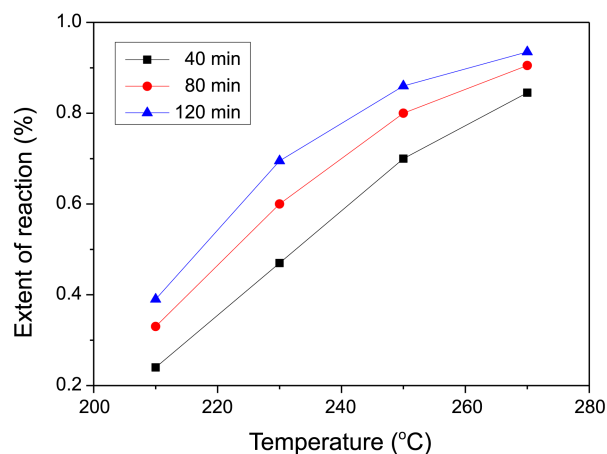
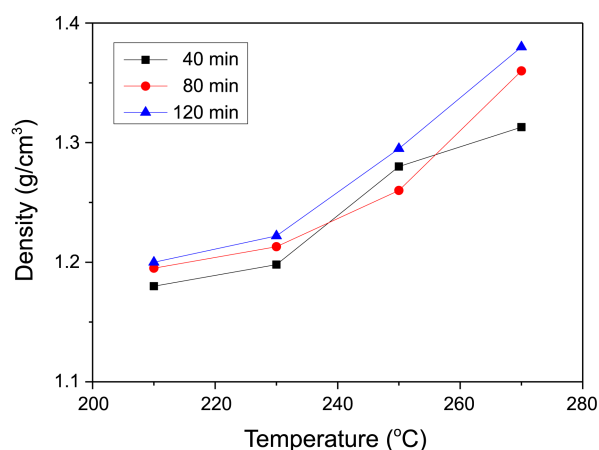
<sup>a</sup>before stabilization. <sup>b</sup>after stabilization.**Figure 5.** X-ray diffraction patterns of PAN ultrafine fibers as a function of draw ratio.

crystal size of the fibers prepared by PVA removal using water increased with 5 wt % water and then decreased with 10 wt % water, which demonstrates that the PVA removal is not significantly affected by the crystal size. After stabilization, the AI value, which was calculated from the peak intensities at  $2\theta = 17$  and  $25.5^\circ$  was 54-55%; this indicates that the permeation of the PVA oligomer into the PAN fiber does not hinder the formation of the fibril structure.<sup>21</sup>

Figure 5 shows the XRD patterns of PAN ultrafine fibers prepared using methanol at draw ratios of 15 and 20 after stabilization or carbonization. The AI value after stabilization was 45-47%, which does not differ significantly from the above results. After carbonization, the peak of the (002) plane at  $2\theta = 25.5^\circ$  increased while the peak of the (101) plane at  $2\theta = 43^\circ$  decreased, which indicates carbonization. The crystal size at  $2\theta = 25.5^\circ$  was 0.225-0.233 nm due to the contraction of fibers as a result of the decreased tension from changes in the crystal arrangements during carbonization.<sup>22</sup>

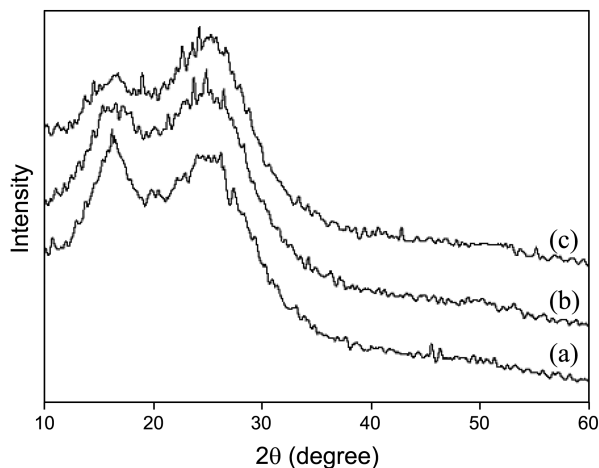
From the above results, it is evident that the PAN ultrafine fibers can be converted to ultrafine carbon fibers through oxidative stabilization and carbonization. Shrinkage affects the crystal arrangement of the final carbon fibers.

**Characterization of the PAN Carbon Fibers.** Figure 6 shows the EOR values of the PAN carbon fibers that were calculated from the FT-IR spectra as functions of the stepwise temperature and dwell time. The EOR is maximized at  $230^\circ\text{C}$  because of the chemical shrinkage that is induced by cyclization of the PAN fibers. At various temperatures, the

**Figure 6.** Extent of reaction as functions of stepwise temperature and dwell time.**Figure 7.** Changes of density as functions of stepwise temperature and dwell time.

EOR increased with increased dwell time.<sup>23</sup>

Figure 7 shows the changes of density as a function of the stepwise temperature and dwell time. The density increased significantly above  $230^\circ\text{C}$  because of the chemical shrinkage

**Figure 8.** X-ray diffraction patterns of stabilized PAN fibers with difference tension at dwell time of 80 min: (a) 3 g; (b) 10 g; (c) 25 g.

**Table 2.** Properties of PAN precursor and resultant carbon fibers

Sample	Tensile strength (MPa)	Tensile modulus (GPa)	Extension (%)	Density (g/cm <sup>3</sup> )	Diameter (μm)
PAN precursor	459.6	11.6	9.2	1.167	10.92
Carbon fibers	2395.8	212.6	1.1	1.735	8.51

that is induced by cyclization of the PAN fibers.

Figure 8 shows the X-ray diffraction patterns of stabilized PAN carbon fibers as a function of tension at a dwell time of 80 min. The tension of the fibers was maintained during the stabilization process, which increases the order of the polymer chains and cross-linking between the chains when chemical shrinkage occurred; this improves the properties of the final carbon fibers. As additional tension was added, the peak intensity at  $2\theta = 17^\circ$  gradually decreased while that at  $2\theta = 25.5^\circ$  increased. The AI values for tensions of 3, 10, and 25 g were 48.15, 53.39, and 54.00%, respectively. Lowering the tension during chemical shrinkage reduces the arrangement of the polymer chain resulting in a lower AI value.<sup>24</sup>

Table 2 shows the properties of the PAN precursor and carbon fibers. The tensile strength and modulus of the carbon fibers of 2396 MPa and 213 GPa, respectively, are much higher than those of PAN precursor.<sup>25,26</sup> These results indicate that the PAN carbon fibers may be suitable for a wide range of applications in carbon papers.

### Conclusions

PAN ultrafine fibers and carbon fibers were produced by wet-spinning, and their crystal sizes and thermal and mechanical properties were investigated. The diameter of the PAN/PVA blend fibers decreased with decreasing PAN content after the PVA was removed. With increasing PVA content, the exothermic peak temperature of PAN increased and the endothermic peak temperature of PVA decreased. The crystal size of the fibers prepared by PVA removal increased with 5 wt % water and decreased with 10 wt % water. The EOR is maximized at a stepwise temperature of 230 °C. The AI value of the PAN carbon fibers increased with increasing tension. The tensile strength and modulus of the carbon fibers were much higher than those of the PAN precursor. The data reported in this paper suggests that PAN ultrafine fibers and carbon fibers have excellent properties and are promising candidates for carbon-paper applications.

**Acknowledgments.** This work was supported by the Korea CCS R&D Center (KCRC) grant funded by the Korea

government.

### References

- Okamoto, M. *Advanced Fiber Spinning Technology*; Woodhead Publishing Ltd.: Kyoto, 1994.
- Said, S. S.; El-Halfawy, O. M.; El-Gowelli, H. M.; Aloufy, A. K.; Boraie, N. A.; El-Khordagui, L. K. *Eur. J. Pharm. Biopharm.* **2012**, *80*, 85.
- Chen, H. M.; Yu, D. G. *J. Mater. Process. Technol.* **2010**, *210*, 1551.
- Zhang, L.; Hsieh, Y. L. *Carbohydr. Polym.* **2008**, *71*, 196.
- Karacan, İ.; Soy, T. *J. Mol. Struct.* **2013**, *1041*, 29.
- Qin, X.; Lu, Y.; Xiao, H.; Song, Y. *Mater. Lett.* **2012**, *76*, 162.
- Su, C.; Gao, A.; Luo, S.; Xu, L. *Carbon* **2013**, *51*, 436.
- Wang, H.; Guo, Q.; Yang, J.; Liu, Z.; Zhao, Y.; Li, J.; Feng, Z.; Liu, L. *Carbon* **2013**, *56*, 296.
- Mosadegh-Sedghi, S.; Brisson, J.; Rodrigue, D.; Iliuta, M. C. *Sep. Purif. Technol.* **2012**, *96*, 117.
- Vautard, F.; Grappe, H.; Ozcan, S. *Appl. Surf. Sci.* **2013**, *268*, 61.
- Ozcan, S.; Filip, P. *Carbon* **2013**, *62*, 240.
- Medeiros, L. I.; Couto, A. B.; Matsushima, J. T.; Baldan, M. R.; Ferreira, N. G. *Thin Solid Films* **2012**, *520*, 5277.
- Shin, H. K.; Park, M.; Chung, Y. S.; Kim, H. Y.; Jin, F. L.; Choi, H. S.; Park, S. J. *Macromol. Res.* **2013**, *21*, 1241.
- Li, P.; Chen, H. Z.; Chung, T. S. *J. Membrane Sci.* **2013**, *434*, 18.
- Jin, F. L.; Park, S. J. *Polym. Degrad. Stab.* **2012**, *97*, 2148.
- Zhu, L.; Jin, F. L.; Park, S. J. *Bull. Korean Chem. Soc.* **2012**, *33*, 2513.
- Jiang, W.; Jin, F. L.; Park, S. J. *J. Ind. Eng. Chem.* **2012**, *18*, 594.
- Jin, F. L.; Rhee, K. Y.; Park, S. J. *J. Solid State Chem.* **2011**, *184*, 3253.
- Yoo, Y. C.; Kim, H. Y.; Jin, F. L.; Park, S. J. *Macromol. Res.* **2013**, *21*, 687.
- (a) Jin, F. L.; Ma, C. J.; Park, S. J. *Mater. Sci. Eng. A* **2011**, *528*, 8517. (b) Park, M. R.; Choi, Y.; Lee, S. Y.; Kim, H. Y.; Park, S. J. *J. Ind. Eng. Chem.* **2014**, in press.
- Liu, L.; Wang, C.; Zhang, F.; Zhang, L.; Wen, S. *J. Rare Earth* **2012**, *30*, 860.
- Hao, Y.; Liu, F.; Shi, H.; Han, E.; Wang, Z. *Prog. Org. Coat.* **2011**, *71*, 188.
- Kim, S.; Chung, Y. S.; Jin, F. L.; Park, S. J. *Bull. Korean Chem. Soc.* submitted for publication.
- Mahapatra, A.; Mishra, B. G.; Hota, G. *Ceram. Int.* **2011**, *37*, 2329.
- Yoo, Y. C.; Kim, H. Y.; Jin, F. L.; Park, S. J. *Bull. Korean Chem. Soc.* **2012**, *33*, 4137.
- Park, M.; Kim, H. Y.; Jin, F. L.; Lee, S. Y.; Choi, H. S.; Park, S. J. *J. Ind. Eng. Chem.* **2013**, in press.